

ENERGY-PRESERVING SPLITTING INTEGRATORS FOR SAMPLING FROM GAUSSIAN DISTRIBUTIONS WITH HAMILTONIAN MONTE CARLO METHOD

FASMA DIELE*

Abstract. The diffusive behaviour of simple random-walk proposals of many Markov Chain Monte Carlo (MCMC) algorithms results in slow exploration of the state space making inefficient the convergence to a target distribution. Hamiltonian/Hybrid Monte Carlo (HMC), by introducing fictitious momentum variables, adopts Hamiltonian dynamics, rather than a probability distribution, to propose future states in the Markov chain. Splitting schemes are numerical integrators for Hamiltonian problems that may advantageously replace the Störmer-Verlet method within HMC methodology. In this paper a family of stable methods for univariate and multivariate Gaussian distributions, taken as guide-problems for more realistic situations, is proposed. Differently from similar methods proposed in the recent literature, the considered schemes are featured by null expectation of the random variable representing the energy error. The effectiveness of the novel procedures is shown for bivariate and multivariate test cases taken from the literature.

Key words. Hamiltonian Monte Carlo, energy-preserving splitting methods, Gaussian distributions

AMS subject classifications. 65L05, 65C05, 37J05

1. Introduction. In the seminal paper [4], the two main approaches to simulate the distribution of states for a molecular system, i.e. the Markov Chain Monte Carlo (MCMC) originated with the classical paper in [11] and the deterministic one, via Hamiltonian formalism [1], are merged in unique method, originally named *Hybrid Monte Carlo*, hereinafter referred to as *Hamiltonian Monte Carlo* (HMC), taking up the suggestion made by R.M. Neal in [12].

At each step of the Markov chain, HMC requires the numerical integration of a Hamiltonian system of differential equations; typically, the second-order splitting method known as *Störmer-Verlet* or *Leapfrog* algorithm (see, e.g., [9]), is used to carry out such an integration. Whether the above algorithm may be replaced by more efficient alternatives is the question faced by many researchers (see, for example, [8], [14], [6], [16] and references therein). In designing a new algorithm the goal is to enlarge the usable time step in order to explore larger portion of the phase space; however, working in the high-time step regime for long-time simulations induces perturbations in computed probability, dependent on the step size. This bias leads to a distortion in calculated energy averages which produces a high percent of rejections in HCM algorithm.

An element unifying the recent efforts made to propose alternatives to the Störmer-Verlet algorithm (see, for example, [2], [14], [8]), is the analysis of their effectiveness when applied to Gaussian distributions. Needless to say, as already underlined in [2], it makes no practical sense to use a Markov chain algorithm to sample from a Gaussian distribution, as it makes no sense to numerically integrate the harmonic oscillator equations. However, it is a common practice to evaluate the performance of algorithms on simple problems as they represent benchmark for more complex situations.

In this perspective, a novel family of stable methods for HMC for sampling from univariate and multivariate Gaussian distributions is here proposed. All the methods

*Istituto per Applicazioni del Calcolo 'M.Picone', via Amendola 122/D, Bari, Italy
(f.diele@ba.iac.cnr.it).

in the family are featured by zero expectation for the random variable representing the energy error. The novel schemes stem from some energy-preserving splitting methods for Hamiltonian dynamics proposed in [13], here analyzed in the context of HMC. The construction of the novel schemes is preceded by the analysis of the linear maps generated by the application of symplectic and reversible integrators within HMC method. The analysis here performed generalizes the one in [2] in that standard deviations may assume values also different from one; on the other side, it departs from [2], this representing an adding element of novelty, as the quantity responsible for the generation of the error in approximating the Hamiltonian, is here exactly identified. In so doing, when a special class of second order splitting integrators is analyzed, it is possible to choose parameters that makes the resulting methods able to exactly preserve the energy. Of course, the above characteristic is of a overall importance within the HMC procedure as, in their implementation, all the proposals are accepted with a consequent saving of computational time, particularly evident in the case of high-dimensional problems.

The paper is organized as follows: in Section 2 the general framework on sampling from a target distributions throughout the HMC algorithm is recalled and some theoretical and practical implementation details are briefly provided. In Section 3, the general characteristics of linear maps generated by the application of a class of symplectic, reversible integrators on univariate Gaussian distribution are analyzed. The expression for the expectation of the energy error is given and specialized for both the Störmer-Verlet method (Subsection 3.1) and for a class of second order splitting integrators in Subsection 3.2. For the last class, the main result is described in Theorem 3.6 where a suitable selection of parameters detects a modified dynamics whose approximated values nullify the expectation of the energy error. This result is then generalized for multivariate Gaussian distributions in Section 4 by Theorem 4.1. Finally, in Section 5, some numerical tests on the application of the proposed procedure for bivariate and multivariate distributions are shown. In Section 6 conclusive remarks and some insights on possible applications of the described results to generic target distributions are drawn.

2. The Hamiltonian Monte Carlo algorithm. The description of HMC algorithm given below follows the steps described in [12]. Given a set of data G , suppose that we wish to sample, using Hamiltonian dynamics, the variable $\mathbf{q} \in \mathbf{R}^d$ from a probability distribution of interest $P(\mathbf{q})$ with prior density $\pi(\mathbf{q})$ and likelihood function $L(\mathbf{q}|G)$ i.e. $P(\mathbf{q}) = \pi(\mathbf{q}) L(\mathbf{q}|G)$. The first step is to associate, via the canonical distribution (measured in units that makes the temperature be equal one), a potential energy function defined as follows

$$U(\mathbf{q}) = -\log [\pi(\mathbf{q}) L(\mathbf{q}|D)] - \log(Z).$$

so that

$$P(\mathbf{q}) = \frac{1}{Z} \exp(-U(\mathbf{q})).$$

where Z is any suitable positive constant. Then, we introduce auxiliary momentum variables $\mathbf{p} \in \mathbf{R}^d$, independent of \mathbf{q} , specifying the distribution via the kinetic energy function $K(\mathbf{p})$. Current practice with HMC is to use a quadratic kinetic energy

$$K(\mathbf{p}) = \frac{1}{2} \mathbf{p}^T D_\beta^{-1} \mathbf{p}$$

where, without loose of generality we suppose that the components of \mathbf{p} are specified to be independent so that D_β is a diagonal matrix with positive entries β_i^2 , each representing the variance of the i th component p_i of the vector \mathbf{p} . The canonical distribution

$$\mathcal{P}(\mathbf{p}) = \exp(-K(\mathbf{p}))$$

results to be the zero-mean multivariate Gaussian distribution. We denote with $H(\mathbf{q}, \mathbf{p}) = U(\mathbf{q}) + K(\mathbf{p})$ the energy function for the joint state of position \mathbf{q} and momentum \mathbf{p} which defines a joint canonical distribution satisfying

$$\mathcal{P}(\mathbf{q}, \mathbf{p}) = \frac{1}{Z} \exp(-H(\mathbf{q}, \mathbf{p})) = \frac{1}{Z} \exp(-U(\mathbf{q})) \exp(-K(\mathbf{p})) = \mathcal{P}(\mathbf{q}) \mathcal{P}(\mathbf{p}).$$

We see that joint (canonical) distribution for \mathbf{q} and \mathbf{p} factorizes. This means that the two variables are independent, and the canonical distribution $\mathcal{P}(\mathbf{q})$ is independent of $\mathcal{P}(\mathbf{p})$. Therefore, we can use Hamiltonian dynamics to sample from the joint canonical distribution $\mathcal{P}(\mathbf{q}, \mathbf{p})$ and simply ignore the momentum contributions. The introduction of the auxiliary variable \mathbf{p} intends to use Hamiltonian dynamics in order to facilitate the Markov chain path.

Starting from the generation of an initial position state $\mathbf{q}^{(i)} \propto \pi(\mathbf{q})$, for $i = 0, \dots, L$ each iteration of HMC algorithm has two step. The first chooses the initial momentum by randomly drawing values $\mathbf{p}^{(i)}$ from its zero-mean multivariate Gaussian distribution $\mathcal{N}(0, D_\beta)$. In the second step, starting at $t = 0$ with initial states $\mathbf{Q}(0) = \mathbf{q}^{(i)}$ and $\mathbf{P}(0) = \mathbf{q}^{(i)}$ it solves the Hamiltonian dynamics

$$(2.1) \quad \frac{d\mathbf{Q}}{dt} = \nabla_{\mathbf{P}} K(\mathbf{P}) = D_\beta^{-1} \mathbf{P}, \quad \frac{d\mathbf{P}}{dt} = -\nabla_{\mathbf{Q}} U(\mathbf{Q}), \quad t \in (0, T^*].$$

Then, the state of the position at the end of the simulation $\mathbf{Q}(T^*)$ is used as the next state of the Markov chain by setting $\mathbf{q}^{(i+1)} = \mathbf{Q}(T^*)$. Combining these steps, sampling random momentum, followed by Hamiltonian dynamics defines the theoretical HMC [Algorithm 2.1](#) for drawing L samples from a target distribution.

Algorithm 2.1 HMC algorithm (theoretical)

```

Draw  $\mathbf{q}^{(1)} \sim \pi(\mathbf{q})$ ,  $\mathbf{q}^{(1)} \in \mathbb{R}^d$ ,  $L \geq 1$ , set  $i = 0$ 
while  $i < L$  do
   $i = i + 1$ 
  Draw  $\mathbf{p}^{(i)} \sim \mathcal{N}(0, D_\beta)$ ,
  Set  $(\mathbf{Q}(0), \mathbf{P}(0)) = (\mathbf{q}^{(i)}, \mathbf{p}^{(i)})$ , set  $j = 0$ 
  while  $j < 1$  do
    Randomly choose  $T^* > 0$ 
    Solve  $\frac{d\mathbf{Q}}{dt} = D_\beta^{-1} \mathbf{P}$ ,  $\frac{d\mathbf{P}}{dt} = -\nabla_{\mathbf{Q}} U(\mathbf{Q})$ ,  $t \in (0, T^*]$ 
    if  $(\mathbf{Q}(T^*), \mathbf{P}(T^*)) \neq (\mathbf{Q}(0), \mathbf{P}(0))$ ,  $j = 1$ 
  end while
  Update:  $\mathbf{q}^{(i+1)} = \mathbf{Q}(T^*)$ 
end while
return Markov chain  $\mathbf{q}^{(1)}, \mathbf{q}^{(2)}, \dots, \mathbf{q}^{(L)}$ 

```

An important observation is that in the framework of Hamiltonian dynamics for the Markov Chain Monte Carlo algorithm, the fictitious final time $T^* > 0$ behaves as a parameter to be selected. A criterium adopted to select this value should preserve the

ergodicity of HMC algorithm. In an HCM iteration, any value can be sampled for the momentum variables, which can typically then affect the position variables in arbitrary ways; however, ergodicity can fail if the chosen T^* produces an exact periodicity for some function of state. For example, with $q^{(i)} \sim \mathcal{N}(0, 1)$ and $p^{(i)} \sim \mathcal{N}(0, 1)$, the Hamiltonian dynamics for Q and P define the equations of harmonic oscillator

$$(2.2) \quad \frac{dQ}{dt} = P, \quad \frac{dP}{dt} = -Q,$$

whose solutions are periodic with period 2π . Choosing $T^* = 2\pi$ the trajectory returns to the same position coordinate and HCM will be not ergodic. This potential problem of non-ergodicity can be solved by randomly choosing T^* and doing this routinely, as in [Algorithm 2.1](#). Of course, even when exact periodicity can be prevented, near periodicity might still slow HCM considerably [[12](#)].

Starting from $\mathbf{Q}_0 = \mathbf{Q}(0)$, $\mathbf{P}_0 = \mathbf{P}(0)$, a practical implementation of the above algorithm needs to numerically integrate the Hamiltonian system (2.1) by means of a map $(\mathbf{Q}_{n+1}, \mathbf{P}_{n+1}) = \Psi_h(\mathbf{Q}_n, \mathbf{P}_n)$, for $n = 0, \dots, N$, where N and the stepsize h satisfy $Nh = T^*$. In order to safely replace the theoretical solution with an approximated one, the chosen map Ψ_h should result a transformation in phase space which inherits, from the theoretical flow, two main characteristic: to be volume-preserving i.e.

$$\det(\Psi'_h(\mathbf{Q}_n, \mathbf{P}_n)) = 1,$$

Ψ' denoting the Jacobian matrix of Ψ , and *momentum flip - reversible* [[5](#)]:

$$\Psi_h(\mathbf{Q}_n, \mathbf{P}_n) = (\mathbf{Q}_{n+1}, \mathbf{P}_{n+1}) \iff \Psi_h(\mathbf{Q}_{n+1}, -\mathbf{P}_{n+1}) = (\mathbf{Q}_n, -\mathbf{P}_n)$$

for $n = 0, \dots, N$. This guarantees the construction of a Markov chain which is reversible with respect to the target probability distribution $\pi(\mathbf{q})$ [[2](#)].

Position and momentum variables at the end of the simulation are used as proposed variables $\mathbf{q}^* = \mathbf{Q}(T^*)$ and $\mathbf{p}^* = \mathbf{P}(T^*)$ and are accepted using an update rule analogous to the Metropolis acceptance criterion. Specifically, if the probability of the joint distribution at T^* i.e. $\exp(-H(\mathbf{q}^*, \mathbf{p}^*))$ is greater than the initial $\exp(-H(\mathbf{q}^{(i)}, \mathbf{p}^{(i)}))$, then the proposed state is accepted randomly and $\mathbf{q}^{(i+1)} = \mathbf{q}^*$, otherwise it is rejected and the next state of the Markov chain is set as $\mathbf{q}^{(i+1)} = \mathbf{q}^{(i)}$. Combining these steps, sampling random momentum, followed by Hamiltonian dynamics and Metropolis acceptance criterion, defines the HMC [Algorithm 2.2](#) for drawing L samples from a target distribution.

Notice that, a map which approximates the solution of the Hamiltonian flow (2.1), in such a way that $H(\mathbf{Q}_N, \mathbf{P}_N) - H(\mathbf{Q}_0, \mathbf{P}_0) \leq 0$ would produce all accepted proposals. However, in [[2](#)] has been shown that, roughly speaking, for a momentum-flip reversible volume-preserving transformation the phase space is always be divided into two regions of the same volume, one corresponding to negative energy errors and the other, corresponding to flip the momentum with positive energy errors, so that, unless the map is energy-preserving it will potentially may lead to rejections.

As the selection of the parameter T^* in order to assure the HCM algorithm to be ergodic is important, the chosen time-stepping $h > 0$ is also crucial in the implementation of [Algorithm 2.2](#). Too small a stepsize will waste computation time as it will require a large N in order to reach the final step $T^* = Nh$. Too large a stepsize will increase bounded oscillations in the value of the Hamiltonian, which would be constant if the trajectory were simulated by an energy-preserving map. When values for h are chosen above the critical stability threshold which is characteristic of

Algorithm 2.2 HMC algorithm (practical)

```

Draw  $\mathbf{q}^{(1)} \sim \pi(\mathbf{q})$ ,  $\mathbf{q}^{(1)} \in \mathbb{R}^d$ ,  $L \geq 1$ , set  $i = 0$ 
while  $i < L$  do
  i=i+1
  Draw  $\mathbf{p}^{(i)} \sim \mathcal{N}(0, D_\beta)$ 
  Set  $(\mathbf{Q}_0, \mathbf{P}_0) = (\mathbf{q}^{(i)}, \mathbf{p}^{(i)})$ , set  $j = 0$ 
  while  $j < 1$  do
    Randomly choose  $T^* > 0$ .
    Set  $N \geq 1$  or  $h > 0$  such that  $T^* = N h$ 
    Evaluate  $(\mathbf{Q}_{n+1} \mathbf{P}_{n+1}) = \Psi_h(\mathbf{Q}_n, \mathbf{P}_n)$ , for  $n = 0, \dots, N-1$ 
    if  $(\mathbf{Q}_N, \mathbf{P}_N) \neq (\mathbf{Q}_0, \mathbf{P}_0)$ ,  $j=1$ 
  end while
  Set  $(\mathbf{q}^*, \mathbf{p}^*) = (\mathbf{Q}_N, \mathbf{P}_N)$ 
  Calculate  $\alpha = \min(1, \exp(H(\mathbf{q}^{(i)}, \mathbf{p}^{(i)}) - H(\mathbf{q}^*, \mathbf{p}^*)))$ 
  Draw  $u \sim \mathcal{U}(0, 1)$ 
  Update: if  $\alpha > u$  then  $\mathbf{q}^{(i+1)} = \mathbf{q}^*$ ; otherwise  $\mathbf{q}^{(i+1)} = \mathbf{q}^{(i)}$ 
end while
return Markov chain  $\mathbf{q}^{(1)}, \mathbf{q}^{(2)}, \dots, \mathbf{q}^{(L)}$ 

```

each approximating map Ψ_h , then the Hamiltonian grows without bound, this resulting, in turns, in an extremely low acceptance rate for states proposed by simulating trajectories.

Classically, the map implemented within a HMC algorithm, is the Störmer-Verlet method. Several attempts to introduce more accurate maps, where *accuracy* is referred to the performance of the map within the HCM algorithm rather than to the accuracy in approximating the dynamical flow, can be found in literature. For a broader view of HMC algorithm, the chapter *MCMC using Hamiltonian dynamics* by R.M. Neal's in [12] is an enlightening reading.

3. Linear test problem: univariate Gaussian distribution. As we mentioned, the selection of the stepsize h should obey to stability constraints. The issue of stability is traditionally faced by means of a test problem; for HCM flows, it is represented by the one-dimensional problem defined by with Gaussian zero-mean distribution for both q and p . Here we generalize the approach in both [2] and [12] by considering generic standard deviations, α for q and β for p , with zero correlation. The Hamiltonian dynamics for Q and P define the equations

$$(3.1) \quad \frac{dQ}{dt} = \frac{P}{\beta^2}, \quad \frac{dP}{dt} = -\frac{Q}{\alpha^2}.$$

Setting $\mathbf{Y} = [Q, P]^T$, the Hamiltonian can be expressed as $H(\mathbf{Y}) = \frac{1}{2} \mathbf{Y}^T \mathcal{D}^{-1} \mathbf{Y} = \frac{1}{2} \left(\frac{Q^2}{\alpha^2} + \frac{P^2}{\beta^2} \right)$ where $\mathcal{D} = \begin{bmatrix} \alpha^2 & 0 \\ 0 & \beta^2 \end{bmatrix}$. Starting from Q_0, P_0 , the theoretical solution at $t_n = n h$ is represented as a linear map $\mathbf{Y}(t_n) = \mathcal{F}^{(n \tilde{h}, \sigma)} \mathbf{Y}_0$, where

$$(3.2) \quad \mathcal{F}^{(n \tilde{h}, \sigma)} = \begin{bmatrix} \cos(n \tilde{h}) & \sigma \sin(n \tilde{h}) \\ -\sigma^{-1} \sin(n \tilde{h}) & \cos(n \tilde{h}) \end{bmatrix}, \quad \tilde{h} = \frac{h}{\alpha \beta}, \quad \sigma = \frac{\alpha}{\beta}.$$

Notice that Hamiltonian can be expressed as $H(\mathbf{Y}) = \frac{1}{2\alpha\beta} \left(\frac{Q^2}{\sigma} + \sigma P^2 \right)$.

We mentioned that the numerical map used to replace the theoretical solution with an approximation should result volume-preserving (here symplectic) and momentum flip-reversible. Both characteristics border our interest to the class of integrators that, when applied to the test problem (3.1), can be expressed as

$$\mathbf{Y}_{n+1} = \mathcal{M}^{(\tilde{h}, \sigma)} \mathbf{Y}_n$$

where $\mathcal{M}^{(\tilde{h}, \sigma)}(1, 1) = \mathcal{M}^{(\tilde{h}, \sigma)}(2, 2)$ and $\det(\mathcal{M}^{(\tilde{h}, \sigma)}) = 1$.

Setting $p_{\tilde{h}} = \mathcal{M}^{(\tilde{h}, \sigma)}(1, 1) = \mathcal{M}^{(\tilde{h}, \sigma)}(2, 2)$, $q_{\tilde{h}} = \frac{\sigma}{\sigma^2 + 1} (\mathcal{M}^{(\tilde{h}, \sigma)}(1, 2) - \mathcal{M}^{(\tilde{h}, \sigma)}(2, 1))$ and $e_{\tilde{h}} = \frac{1}{\sigma^2 + 1} (\mathcal{M}^{(\tilde{h}, \sigma)}(1, 2) + \sigma^2 \mathcal{M}^{(\tilde{h}, \sigma)}(2, 1))$, the matrix $\mathcal{M}^{(\tilde{h}, \sigma)}$ can be written as

$$(3.3) \quad \mathcal{M}^{(\tilde{h}, \sigma)} = \begin{bmatrix} p_{\tilde{h}} & e_{\tilde{h}} + \sigma q_{\tilde{h}} \\ e_{\tilde{h}} - \sigma^{-1} q_{\tilde{h}} & p_{\tilde{h}} \end{bmatrix},$$

and, from $\det(\mathcal{M}^{(\tilde{h}, \sigma)}) = 1$, the following relation holds

$$(3.4) \quad p_{\tilde{h}}^2 - (e_{\tilde{h}} + \sigma q_{\tilde{h}})(e_{\tilde{h}} - \sigma^{-1} q_{\tilde{h}}) = 1.$$

The stability of the trajectories depends on eigenvalues of $\mathcal{M}^{(\tilde{h}, \sigma)}$ which solve the polynomial

$$\lambda^2 - 2p_{\tilde{h}}\lambda + 1 = 0.$$

When $p_{\tilde{h}}^2 - 1 \geq 0$ then the eigenvalues are real with at least one will have absolute value grater than one, hence trajectories are unstable. When $p_{\tilde{h}}^2 - 1 < 0$ the eigenvalues are complex with modulus equal to one, hence trajectories are stable.

The key consideration for what follows is that integrators for which it results $e_{\tilde{h}} = 0$ are energy preserving. Indeed, the error in energy at each step is given by

$$\begin{aligned} \Delta_h^{(n)} &= H(\mathbf{Y}_{n+1}) - H(\mathbf{Y}_n) = \frac{1}{2} \mathbf{Y}_{n+1}^T \mathcal{D}^{-1} \mathbf{Y}_{n+1} - \frac{1}{2} \mathbf{Y}_n^T \mathcal{D}^{-1} \mathbf{Y}_n \\ &= \frac{1}{2} \mathbf{Y}_n^T \mathcal{M}^{(\tilde{h}, \sigma)}^T \mathcal{D}^{-1} \mathcal{M}^{(\tilde{h}, \sigma)} \mathbf{Y}_n - \frac{1}{2} \mathbf{Y}_n^T \mathcal{D}^{-1} \mathbf{Y}_n \\ &= \frac{1}{2} \mathbf{Y}_n^T \left(\mathcal{M}^{(\tilde{h}, \sigma)}^T \mathcal{D}^{-1} \mathcal{M}^{(\tilde{h}, \sigma)} - \mathcal{D}^{-1} \right) \mathbf{Y}_n \\ &= \frac{1}{2} \mathbf{Y}_n^T (\mathcal{K}_{\tilde{h}}^T \mathcal{K}_{\tilde{h}} - \mathcal{D}^{-1}) \mathbf{Y}_n \end{aligned}$$

where $\mathcal{K}_{\tilde{h}} = \mathcal{D}^{-1/2} \mathcal{M}^{(\tilde{h}, \sigma)} = \begin{pmatrix} \frac{p_{\tilde{h}}}{\alpha} & \frac{e_{\tilde{h}}}{\alpha} + \frac{q_{\tilde{h}}}{\beta} \\ \frac{e_{\tilde{h}}}{\beta} - \frac{q_{\tilde{h}}}{\alpha} & \frac{p_{\tilde{h}}}{\beta} \end{pmatrix}$. Let us evaluate

$$(3.5) \quad \mathcal{E}_{\tilde{h}} = \mathcal{K}_{\tilde{h}}^T \mathcal{K}_{\tilde{h}} - \mathcal{D}^{-1} = \begin{pmatrix} \frac{p_{\tilde{h}}^2 - 1}{\alpha^2} + \left(\frac{e_{\tilde{h}}}{\beta} - \frac{q_{\tilde{h}}}{\alpha} \right)^2 & \left(\frac{1}{\alpha^2} + \frac{1}{\beta^2} \right) e_{\tilde{h}} p_{\tilde{h}} \\ \left(\frac{1}{\alpha^2} + \frac{1}{\beta^2} \right) e_{\tilde{h}} p_{\tilde{h}} & \frac{p_{\tilde{h}}^2 - 1}{\beta^2} + \left(\frac{e_{\tilde{h}}}{\alpha} + \frac{q_{\tilde{h}}}{\beta} \right)^2 \end{pmatrix}$$

so that $\Delta_h^{(n)} := H(\mathbf{Y}_{n+1}) - H(\mathbf{Y}_n) = \frac{1}{2} \mathbf{Y}_n^T \mathcal{E}_{\tilde{h}} \mathbf{Y}_n$, for $n = 0, \dots, N$ and

$$\Delta_N = H(\mathbf{Y}_N) - H(\mathbf{Y}_0) = \sum_{n=0}^N \Delta_h^{(n)} = \frac{1}{2} \sum_{n=0}^N \mathbf{Y}_n^T \mathcal{E}_{\tilde{h}} \mathbf{Y}_n.$$

THEOREM 3.1. *Consider the Hamiltonian test problem (3.1) and a symplectic and momentum flip - reversible integrator which can be expressed as $\mathbf{Y}_{n+1} = \mathcal{M}^{(\tilde{h}, \sigma)} \mathbf{Y}_n$ with $\mathcal{M}^{(\tilde{h}, \sigma)}$ defined in (3.3), when applied to (3.1). If it results that $e_{\tilde{h}} = 0$, then the integrator preserves the Hamiltonian.*

Proof. It is enough to observe that, whenever $e_{\tilde{h}} = 0$, the matrix $\mathcal{E}_{\tilde{h}}$ in (3.5) has null entries on the right-left diagonal. From relation (3.4), it follows that on the principal diagonal $\mathcal{E}_{\tilde{h}}(1,1) = \frac{p_{\tilde{h}}^2 + q_{\tilde{h}}^2 - 1}{\alpha^2} = \mathcal{E}_{\tilde{h}}(2,2) = \frac{p_{\tilde{h}}^2 + q_{\tilde{h}}^2 - 1}{\beta^2} = 0$ which completes the proof. \square

THEOREM 3.2. *Assume that Q_0, P_0 are two random variables with Gaussian zero-mean distribution, standard deviations α and β respectively and zero correlation. Suppose that the Hamiltonian dynamics (3.1) is approximated by means of a linear map $\mathbf{Y}_{n+1} = \mathcal{M}^{(\tilde{h}, \sigma)} \mathbf{Y}_n$ with $\mathcal{M}^{(\tilde{h}, \sigma)}$ given in (3.3). Then, the expectation of the random variable $\Delta_N = H(\mathbf{Y}_N) - H(\mathbf{Y}_0) = \sum_{n=0}^{N-1} \Delta_h^{(n)}$ is given by*

$$\mathbb{E}(\Delta_N) = \frac{N}{2} \left(\sigma + \frac{1}{\sigma} \right)^2 e_{\tilde{h}}^2$$

and, consequently, $\mathbb{E}(\Delta_N) = 0$ if $e_{\tilde{h}} = 0$.

Proof. From $\Delta_h^{(n)} = \frac{1}{2} \mathbf{Y}_n^T \mathcal{E}_{\tilde{h}} \mathbf{Y}_n$, we can evaluate

$$\begin{aligned} 2 \Delta_h^{(n)} &= \left[\frac{p_{\tilde{h}}^2 - 1}{\alpha^2} + \left(\frac{e_{\tilde{h}}}{\beta} - \frac{q_{\tilde{h}}}{\alpha} \right)^2 \right] Q_0^2 + 2 e_{\tilde{h}} p_{\tilde{h}} \left(\frac{1}{\alpha^2} + \frac{1}{\beta^2} \right) Q_0 P_0 \\ &+ \left[\frac{p_{\tilde{h}}^2 - 1}{\beta^2} + \left(\frac{e_{\tilde{h}}}{\alpha} + \frac{q_{\tilde{h}}}{\beta} \right)^2 \right] P_0^2 \end{aligned}$$

for $n = 0, \dots, N$. From $\mathbb{E}(Q_0^2) = \alpha^2$, $\mathbb{E}(P_0^2) = \beta^2$, $\mathbb{E}(Q_0 P_0) = 0$, it results that

$$2 \mathbb{E}(\Delta_h^{(n)}) = 2(p_{\tilde{h}}^2 - 1) + (\sigma e_{\tilde{h}} - q_{\tilde{h}})^2 + (\sigma^{-1} e_{\tilde{h}} + q_{\tilde{h}})^2 = (\sigma e_{\tilde{h}} + \sigma^{-1} e_{\tilde{h}})^2$$

and the statement trivially follows. \square

Finally, we underline that, under conditions which assures the stability of their trajectories (i.e. $p_{\tilde{h}}^2 - 1 < 0$), the discrete map $\mathbf{Y}_h = \mathcal{M}^{(\tilde{h}, \sigma)} \mathbf{Y}_0$ corresponding to the application of a symplectic momentum-flip reversible integrator to the the test model (3.1), provides the exact solutions of a modified Hamiltonian dynamics. Indeed, it is possible to define two shadow variances x_h^2 and y_h^2 such that, by setting $\theta_h = \frac{h}{x_h y_h}$ and $\chi_h = \frac{x_h}{y_h}$, it results $\mathcal{F}^{(\theta_h, \chi_h)} = \mathcal{M}^{(\tilde{h}, \sigma)}$. To this aim, θ_h and χ_h should satisfy the following equations:

$$\begin{cases} p_{\tilde{h}} = \cos \theta_h \\ e_{\tilde{h}} + \sigma q_{\tilde{h}} = \chi_h \sin \theta_h \\ e_{\tilde{h}} - \sigma^{-1} q_{\tilde{h}} = -\chi_h^{-1} \sin \theta_h \end{cases}$$

Form the first equation $\theta_h = \arccos p_{\tilde{h}}$, $\theta_h \in [0, \pi]$ and $\sin \theta_h = \sqrt{1 - p_{\tilde{h}}^2}$. Second and third equations give $\chi_h = \frac{e_{\tilde{h}} + \sigma q_{\tilde{h}}}{\sqrt{1 - p_{\tilde{h}}^2}} = \frac{\sqrt{1 - p_{\tilde{h}}^2}}{\sigma^{-1} q_{\tilde{h}} - e_{\tilde{h}}}$, equality which is satisfied by relation (3.4). Finally, $x_h^2 = \frac{h \chi_h}{\theta_h}$, and $y_h^2 = \frac{h}{\theta_h \chi_h}$ so that, setting $\mathcal{D}_h = \begin{bmatrix} \frac{h \chi_h}{\theta_h} & 0 \\ 0 & \frac{h}{\theta_h \chi_h} \end{bmatrix}$ the modified Hamiltonian $\tilde{H}(\mathbf{Y})$ is conserved at each step i.e.

$$(3.6) \quad \tilde{H}(\mathbf{Y}_N) = \cdots = \tilde{H}(\mathbf{Y}_0) = \frac{1}{2} \mathbf{Y}_0^T \mathcal{D}_h^{-1} \mathbf{Y}_0 = \frac{\theta_h}{2h} \left(\frac{Q_0^2}{\chi_h} + \chi_h P_0^2 \right),$$

where

$$\mathbf{Y}_{n+1} = \mathcal{F}^{(\theta_h, \chi_h)} \mathbf{Y}_n = \begin{bmatrix} \cos(\theta_h) & \chi_h \sin(\theta_h) \\ -\chi_h^{-1} \sin(\theta_h) & \cos(\theta_h) \end{bmatrix} \mathbf{Y}_n,$$

for $n = 0, \dots, N-1$.

The following result generalizes Proposition 4.3 in [2] for Gaussian zero-mean distribution with generic standard deviations α and β :

THEOREM 3.3. *In the same hypothesis of Theorem 3.1, in case when $|\mathcal{M}^{(\tilde{h}, \sigma)}| < 1$, the expectation of the random variable $\Delta_N = H(\mathbf{Y}_N) - H(\mathbf{Y}_0) = \sum_{n=0}^{N-1} \Delta_h^{(n)}$ can be expressed as*

$$\mathbb{E}(\Delta_N) = N \sin^2(\theta_h) \rho(h), \quad \rho(h) = \frac{1}{2} \left(\tilde{\chi}_h - \frac{1}{\tilde{\chi}_h} \right)^2, \quad \tilde{\chi}_h = \frac{\chi_h}{\sigma}.$$

Proof. Under the assumption $|\mathcal{M}^{(\tilde{h}, \sigma)}| < 1$, then $|\mathbf{p}_{\tilde{h}}| < 1$ and it is possible to define $\theta_h = \arccos \mathbf{p}_{\tilde{h}}$, $\theta_h \in [0, \pi]$ and $\sin \theta_h = \sqrt{1 - \mathbf{p}_{\tilde{h}}^2}$. The relation $\sin^2(\theta_h) = 1 - \mathbf{p}_{\tilde{h}}^2$, the definitions

$$\chi_h = \frac{\mathbf{e}_{\tilde{h}} + \sigma \mathbf{q}_{\tilde{h}}}{\sqrt{1 - \mathbf{p}_{\tilde{h}}^2}}, \quad \frac{1}{\chi_h} = \frac{\sigma^{-1} \mathbf{q}_{\tilde{h}} - \mathbf{e}_{\tilde{h}}}{\sqrt{1 - \mathbf{p}_{\tilde{h}}^2}},$$

and relation (3.4) allow to prove that

$$2 \sin^2(\theta_h) \rho(h) = \sin^2(\theta_h) \left(\frac{\chi_h}{\sigma} - \frac{\sigma}{\chi_h} \right)^2 = \left(\sigma + \frac{1}{\sigma} \right)^2 \mathbf{e}_{\tilde{h}}^2.$$

From Theorem 3.2 the result follows. \square

Remark 1. In case when $\mathbf{e}_{\tilde{h}}^2 = 0$, it results $\chi_h = \sigma$ and the modified Hamiltonian in (3.6) can be written as $\frac{\theta_h}{2\tilde{h}} \left(\frac{Q^2}{\sigma} + \sigma P^2 \right)$. Comparing this expression with the expression of the true Hamiltonian $\frac{1}{2\alpha\beta} \left(\frac{Q^2}{\sigma} + \sigma P^2 \right)$ we see that phase-error depends on the approximation $\theta_h \approx \tilde{h} = \frac{h}{\alpha\beta}$

Remark 2. Theorem 3.2 can be also proved by means of a direct verification as in [2]. This means to evaluate

$$\begin{aligned} 2\Delta_h^{(n)} &= 2(H(\mathbf{Y}_{n+1}) - H(\mathbf{Y}_n)) = \mathbf{Y}_{n+1}^T \mathcal{D}^{-1} \mathbf{Y}_{n+1} - \mathbf{Y}_n^T \mathcal{D}^{-1} \mathbf{Y}_n \\ &= \mathbf{Y}_n^T \mathcal{F}^{(\theta_h, \chi_h)}^T \mathcal{D}^{-1} \mathcal{F}^{(\theta_h, \chi_h)} \mathbf{Y}_n - \mathbf{Y}_n^T \mathcal{D}^{-1} \mathbf{Y}_n \\ &= \mathbf{Y}_n^T \left(\mathcal{F}^{(\theta_h, \chi_h)}^T \mathcal{D}^{-1} \mathcal{F}^{(\theta_h, \chi_h)} - \mathcal{D}^{-1} \right) \mathbf{Y}_n \end{aligned}$$

where $\tilde{\mathcal{E}}_h = \mathcal{F}^{(\theta_h, \chi_h)}^T \mathcal{D}^{-1} \mathcal{F}^{(\theta_h, \chi_h)} - \mathcal{D}^{-1}$ is given by

$$(3.7) \quad \tilde{\mathcal{E}}_h = \begin{pmatrix} s^2 \left(\frac{1}{\beta^2 \chi_h^2} - \frac{1}{\alpha^2} \right) & 2cs \left(\frac{\chi_h}{\alpha^2} - \frac{1}{\beta^2 \chi_h} \right) \\ 2cs \left(\frac{\chi_h}{\alpha^2} - \frac{1}{\beta^2 \chi_h} \right) & s^2 \left(\frac{\chi_h^2}{\alpha^2} - \frac{1}{\beta^2} \right) \end{pmatrix}$$

with $c = \cos(\theta_h)$ and $s = \sin(\theta_h)$, so that

$$2\Delta_h^{(n)} = s^2 \left(\frac{1}{\beta^2 \chi_h^2} - \frac{1}{\alpha^2} \right) Q_0^2 + 2cs \left(\frac{\chi_h}{\alpha^2} - \frac{1}{\beta^2 \chi_h} \right) Q_0 P_0 + s^2 \left(\frac{\chi_h^2}{\alpha^2} - \frac{1}{\beta^2} \right) P_0^2.$$

Since $\mathbb{E}(Q_0^2) = \alpha^2$, $\mathbb{E}(P_0^2) = \beta^2$, $\mathbb{E}(Q_0 P_0) = 0$, then the result follows.

3.1. Störmer-Verlet method. The Störmer-Verlet method lies in the class of symmetric splitting method as it is based on the splitting of the flow in two (or more) semiflows and is built as a symmetric composition of that semiflows. When applied to Hamiltonian dynamics, the semiflows result themselves Hamiltonian, so that they are volume-preserving and reversible maps. The composition of volume-preserving maps results a volume-preserving map; moreover, as the semiflows are reversible and the composition is symmetric, the splitting map results reversible (for a detailed proof see [2]). Having set $\mathbf{Y} = [\mathbf{Q}, \mathbf{P}]^T \in \mathbb{R}^{2d}$, it can be useful to denote the Hamiltonian dynamics (3.8) in vectorial form

$$\frac{d\mathbf{Y}}{dt} = f(\mathbf{Y}) := \left[D_{\beta}^{-1} \mathbf{P}, -\nabla_{\mathbf{Q}} U(\mathbf{Q}) \right]^T.$$

Let $\varphi_t^{[P]}$ and $\varphi_t^{[Q]}$ represent the exact flows associated to the dynamics $\frac{d\mathbf{Y}}{dt} = f^{[P]}(\mathbf{Y})$ and $\frac{d\mathbf{Y}}{dt} = f^{[Q]}(\mathbf{Y})$, where $f = f^{[P]} + f^{[Q]}$ and

$$f^{[P]}(\mathbf{Y}) := [D_{\beta}^{-1} \mathbf{P}, \mathbf{0}_d]^T, \quad f^{[Q]}(\mathbf{Y}) := [\mathbf{0}_d, -\nabla_{\mathbf{Q}} U(\mathbf{Q})]^T.$$

The map $\mathbf{Y}_{n+1} = \Psi_h^{(SV)}(\mathbf{Y}_n)$, with

$$(3.8) \quad \Psi_h^{(SV)} := \varphi_{h/2}^{[Q]} \circ \varphi_h^{[P]} \circ \varphi_{h/2}^{[Q]},$$

defines the (*velocity*) Störmer-Verlet method.¹

A Störmer-Verlet step applied to the linear test problem (3.1) will be a linear map, represented in matrix form as $\mathbf{Y}_{n+1} = \mathcal{M}^{(\tilde{h}, \sigma)} \mathbf{Y}_n$ where $\mathcal{M}^{(\tilde{h}, \sigma)}$ is given in (3.3) and

$$p_{\tilde{h}} = 1 - \frac{\tilde{h}^2}{2}, \quad e_{\tilde{h}} = \frac{\sigma \tilde{h}^3}{4(\sigma^2 + 1)}, \quad q_{\tilde{h}} = \tilde{h} - \sigma^{-1} e_{\tilde{h}},$$

It results that, for $\tilde{h} \leq 2$, the trajectories are stable as it results $p_{\tilde{h}}^2 - 1 < 0$.

Since $e_{\tilde{h}} \neq 0$, the Störmer-Verlet integrator cannot preserve the energy when applied to the linear test model (3.1). From Theorem 3.2 the expectation of the random variable Δ_N is given by

$$\mathbb{E}(\Delta_N) = \frac{N}{2} \left(\sigma + \frac{1}{\sigma} \right)^2 \left(\frac{\sigma \tilde{h}^3}{4(\sigma^2 + 1)} \right)^2 = \frac{N}{32} \tilde{h}^6 = T^* \left(\frac{\tilde{h}}{2} \right)^5.$$

3.2. A class of second order splitting methods. Different improvements of the Störmer-Verlet method can be found in literature. Often the idea is tuning some free parameter in some suitable class of methods in order to maximizing, for the linear test model, the length of the stability interval, subject to the annihilation of some error constants as [14] or to ensure good conservation of energy properties in linear problems so reducing the energy error as in [2]. In both cases the aim is to suggest

¹We mention that the *position* Störmer-Verlet method starts the integration by solving the semi-flow $f^{[P]}$ so that $\Psi_h^{(SV)} := \varphi_{h/2}^{[P]} \circ \varphi_h^{[Q]} \circ \varphi_{h/2}^{[P]}$.

methods able to increase the number of accepted proposals in HCM algorithm with respect to the Störmer-Verlet method.

In this paper a similar approach is adopted by tuning a free parameter $b \in \mathbb{R}$ in the class of second order splitting methods

$$(3.9) \quad \Psi_h^{(b)} := \varphi_{bh}^{[Q]} \circ \varphi_{h/2}^{[P]} \circ \varphi_{(1-2b)h}^{[Q]} \circ \varphi_{h/2}^{[P]} \circ \varphi_{bh}^{[Q]}.$$

The aim is to exactly preserve the energy so to have all proposals accepted when HCM is applied for univariate Gaussian distribution.

Let us underline that this idea is not novel in the field of numerical approximation of Hamiltonian dynamics [13]. However, the benefits of this approach have not been analyzed in the field of Hamiltonian Monte Carlo algorithms. Before proceeding, as observed in [2], notice that the mapping $\Psi_h^{(b)}$ in (3.9) is volume-preserving, reversible and symplectic. Moreover, we will consider $b \neq 0, 1/2$ as the method reduces to the classical velocity and position Störmer-Verlet integrators.

The class of second order methods $\mathbf{Y}_{n+1} = \Psi_h^{(b)}(\mathbf{Y}_n)$, with $\Psi_h^{(b)}$ given in (3.9) when applied to the model test system (3.1) can be written as a linear map, represented in matrix form as $\mathbf{Y}_{n+1} = \mathcal{M}^{(\tilde{h}, \sigma)} \mathbf{Y}_n$ where $\mathcal{M}^{(\tilde{h}, \sigma)}$ is given in (3.3) and

$$\begin{aligned} p_{\tilde{h}} &= 1 - \frac{\tilde{h}^2}{2} + \frac{\tilde{h}^4}{4} b (1 - 2b), \\ q_{\tilde{h}} &= \frac{b^2(1-2b)}{4(\sigma^2+1)} \tilde{h}^5 + \frac{4b^2 + 2b\sigma^2 - 4b - \sigma^2}{4(\sigma^2+1)} \tilde{h}^3 + \tilde{h}. \end{aligned}$$

and

$$(3.10) \quad e_{\tilde{h}} = e_{\tilde{h}}(b) = \frac{\tilde{h}^3 \sigma}{4(\sigma^2+1)} \left(2b^3 \tilde{h}^2 - b^2 \tilde{h}^2 - 4b^2 + 6b - 1 \right).$$

Stability interval can be deduced from the known result given in [2] i.e.

$$(3.11) \quad 0 < \tilde{h} < \min \left\{ \sqrt{\frac{2}{b}}, \sqrt{\frac{2}{1/2 - b}} \right\}, \quad \tilde{h} = \frac{h}{\alpha \beta}, \quad 0 < b < \frac{1}{2}.$$

The application of Theorem 3.2 gives the expectation of the random variable Δ_N

$$\mathbb{E}(\Delta_N) = T^* \left(\frac{\tilde{h}}{2} \right)^5 \left(2b^3 \tilde{h}^2 - b^2 \tilde{h}^2 - 4b^2 + 6b - 1 \right)^2$$

which can be nullified exploiting the following result which generalizes Theorem 1 given in [13].

THEOREM 3.4. *Let $b_R = b_R(\tilde{h})$ a real root of the third degree polynomial*

$$(3.12) \quad r_{\tilde{h}}(b) = 2\tilde{h}^2 b^3 - (4 + \tilde{h}^2) b^2 + 6b - 1, \quad \tilde{h} = \frac{h}{\alpha \beta},$$

then the scheme $\mathbf{Y}_{n+1} = \Psi_h^{(b_R)}(\mathbf{Y}_n)$, with $\Psi_h^{(b_R)}$ given in (3.9) is energy-preserving for the test model (3.1).

Proof. Write $e_{\tilde{h}}(b)$ in (3.10) as $e_{\tilde{h}}(b) = \frac{\tilde{h}^3 \sigma}{4(\sigma^2 + 1)} r_{\tilde{h}}(b)$; then, $e_{\tilde{h}}(b_R) = 0$. From Theorem 3.1, the result follows. \square

In the HMC framework it can be more useful to adopt a different perspective:

THEOREM 3.5. *Set*

$$(3.13) \quad \Omega = \left\{ (b, h_b) \in \mathbb{R}_+^2, \quad h_b = \sqrt{\frac{4b^2 - 6b + 1}{b^2(2b - 1)}}, \quad \frac{3 - \sqrt{5}}{4} < b < \frac{1}{4} \right\}$$

Then the scheme in (3.9) given by $\mathbf{Y}_{n+1} = \Psi_h^{(b)}(\mathbf{Y}_n)$ with $h = \alpha \beta h_b$ and $(b, h_b) \in \Omega$ provides a stable energy-preserving approximation of the test model (3.1).

Proof. It is enough to consider $r_{\tilde{h}}(b)$ in (3.12) as a second order polynomial with respect to \tilde{h} which admits the positive root h_b given in (3.13), for $\frac{3 - \sqrt{5}}{4} < b < \frac{1}{2}$; as a consequence $e_{h_b}(b) = 0$ and, from Theorem 3.1, the conservation of energy follows. Moreover, under the hypothesis of b bounded by $\frac{1}{4}$ from above, it results

$$h_b \leq \sqrt{\frac{4}{1 - 2b}} = \min \left\{ \sqrt{\frac{2}{b}}, \sqrt{\frac{2}{1/2 - b}} \right\}$$

so that h_b satisfies stability condition (3.11). \square

An important consequence which will be useful in the next Section to extend the described result to the multivariate case, is the following.

THEOREM 3.6. *The scheme $\mathbf{Y}_{n+1} = \tilde{\Psi}_{h_b}^{(b)}(\mathbf{Y}_n)$ with $(b, h_b) \in \Omega$ and*

$$(3.14) \quad \tilde{\Psi}_{h_b}^{(b)} := \tilde{\varphi}_{bh_b}^{[Q]} \circ \tilde{\varphi}_{h_b/2}^{[P]} \circ \tilde{\varphi}_{(1-2b)h_b}^{[Q]} \circ \tilde{\varphi}_{h_b/2}^{[P]} \circ \tilde{\varphi}_{bh_b}^{[Q]}$$

where $\tilde{\varphi}_t^{[P]}$ and $\tilde{\varphi}_t^{[Q]}$ represent the exact flows of the dynamics $\frac{d\mathbf{Y}}{dt} = [\sigma P, \mathbf{0}]^T$ and $\frac{d\mathbf{Y}}{dt} = [\mathbf{0}, -\sigma^{-1}Q]^T$, respectively, provides a stable energy-preserving approximation of the test model (3.1).

Proof. It is enough to observe that the scheme $\mathbf{Y}_{n+1} = \tilde{\Psi}_{h_b}^{(b)}(\mathbf{Y}_n)$ with $(b, h_b) \in \Omega$ is equivalent to the scheme (3.9) given by $\mathbf{Y}_{n+1} = \Psi_h^{(b)}(\mathbf{Y}_n)$ with $h = \alpha \beta h_b$. \square

4. Generalization to multivariate Gaussian distribution. Consider the motion of d oscillators

$$(4.1) \quad \frac{dQ_j}{dt} = \frac{P_j}{\beta_j^2}, \quad \frac{dP_j}{dt} = -\frac{Q_j}{\alpha_j^2}, \quad \text{for } j = 1, \dots, d.$$

In the previous section it was shown how to build a symplectic, reversible, energy-preserving scheme for the j th oscillator (4.1), for $j = 1, \dots, d$. Setting $\mathbf{Y}^{(j)} := [Q_j, P_j]$, consider the scheme $\mathbf{Y}_{n+1}^{(j)} = \tilde{\Psi}_{h_b}^{(b)}(\mathbf{Y}_n^{(j)})$ with

$$(4.2) \quad \tilde{\Psi}_{h_b}^{(b)} := \tilde{\varphi}_{bh_b}^{[Q_j]} \circ \tilde{\varphi}_{h_b/2}^{[P_j]} \circ \tilde{\varphi}_{(1-2b)h_b}^{[Q_j]} \circ \tilde{\varphi}_{h_b/2}^{[P_j]} \circ \tilde{\varphi}_{bh_b}^{[Q_j]}, \quad (b, h_b) \in \Omega,$$

where $\tilde{\varphi}_t^{[P_j]}$ and $\tilde{\varphi}_t^{[Q_j]}$ represent the exact flows of

$$\frac{d\mathbf{Y}^{(j)}}{dt} = [\sigma_j P_j, 0]^T, \quad \frac{d\mathbf{Y}^{(j)}}{dt} = [0, -\sigma_j^{-1} Q_j]^T, \quad \sigma_j = \frac{\alpha_j}{\beta_j},$$

for $j = 1, \dots, d$. It is a symplectic, reversible, stable scheme for the j -th oscillator (4.1), which preserves the j -th Hamiltonian $H_j(Q_j, P_j) = \frac{1}{2} \left(\frac{Q_j^2}{\alpha_j^2} + \frac{P_j^2}{\beta_j^2} \right) = \frac{1}{2 \alpha_j \beta_j} \left(\frac{Q_j^2}{\sigma_j} + \sigma_j P_j^2 \right)$.

Now we are searching for symplectic, reversible, energy-preserving scheme for the d -dimensional system

$$(4.3) \quad \frac{d\mathbf{Q}}{dt} = D_\beta^{-1} \mathbf{P}, \quad \frac{d\mathbf{P}}{dt} = -D_\alpha^{-1} \mathbf{Q}.$$

The Hamiltonian $\frac{1}{2} \mathbf{Q}^T D_\alpha^{-1} \mathbf{Q} + \frac{1}{2} \mathbf{P}^T D_\beta^{-1} \mathbf{P}$ can be written as $H(\mathbf{Y}) = \frac{1}{2} \mathbf{Y}^T \mathcal{D}^{-1} \mathbf{Y}$ where $\mathbf{Y} = [\mathbf{Q}, \mathbf{P}]^T$, $\mathcal{D} = \begin{bmatrix} D_\alpha & \mathbf{0}_d \\ \mathbf{0}_d & D_\beta \end{bmatrix}$ and D_α and D_β are $d \times d$ diagonal matrices with entries α_j^2 and β_j^2 , respectively, for $j = 1, \dots, d$.

THEOREM 4.1. Define $\Sigma = D_\alpha^{1/2} D_\beta^{-1/2}$. The method $\mathbf{Y}_{n+1} = \tilde{\Psi}_{h_b}^{(b)} \mathbf{Y}_n$ where

$$(4.4) \quad \tilde{\Psi}_{h_b}^{(b)} := \tilde{\varphi}_{bh_b}^{[Q]} \circ \tilde{\varphi}_{h_b/2}^{[P]} \circ \tilde{\varphi}_{(1-2b)h_b}^{[Q]} \circ \tilde{\varphi}_{h_b/2}^{[P]} \circ \tilde{\varphi}_{bh_b}^{[Q]}, \quad (b, h_b) \in \Omega$$

with $\tilde{\varphi}_t^{[P]}$ and $\tilde{\varphi}_t^{[Q]}$ representing the exact flows of

$$\frac{d\mathbf{Y}}{dt} = [\Sigma \mathbf{P}, \mathbf{0}_d]^T, \quad \frac{d\mathbf{Y}}{dt} = [\mathbf{0}_d, -\Sigma^{-1} \mathbf{Q}]^T,$$

provides a symplectic, reversible, stable approximation for the system (4.3), which preserves the Hamiltonian $H(\mathbf{Y}) = \frac{1}{2} \mathbf{Y}^T \mathcal{D}^{-1} \mathbf{Y}$.

Proof. The method (4.4) can be expressed as $\mathbf{Y}_{n+1} = \mathcal{M}^{(h_b, \Sigma)} \mathbf{Y}_n$ where

$$(4.5) \quad \mathcal{M}^{(h_b, \Sigma)} = \begin{bmatrix} \mathbf{P}_{h_b} & \mathbf{E}_{h_b} + \Sigma \mathbf{Q}_{h_b} \\ \mathbf{E}_{h_b} - \Sigma^{-1} \mathbf{Q}_{h_b} & \mathbf{P}_{h_b} \end{bmatrix},$$

where

$$\mathbf{P}_{h_b} = \left(1 - \frac{h_b^2}{2} + \frac{h_b^4}{4} b (1 - 2b) \right) \mathbf{I}_d,$$

$$\mathbf{Q}_{h_b}(j, j) = \frac{b^2(1-2b)}{4(\sigma_j^2+1)} h_b^5 + \frac{4b^2+2b\sigma_j^2-4b-\sigma_j^2}{4(\sigma_j^2+1)} h_b^3 + h_b,$$

$$\mathbf{E}_{h_b}(j, j) = \frac{h_b^3 \sigma_j}{4(\sigma_j^2+1)} (2b^3 h_b^2 - b^2 h_b^2 - 4b^2 + 6b - 1) = 0,$$

and $Q_{h_b}(i, j) = E_{h_b}(i, j) = 0$ for $i \neq j$, $i, j = 1, \dots, d$.

Similary to the univariate case, the error in energy at each step is given by

$$\Delta_{h_b}^{(n)} = H(\mathbf{Y}_{n+1}) - H(\mathbf{Y}_n) = \frac{1}{2} \mathbf{Y}_n^T \left(\mathcal{K}_{h_b}^{(\Sigma)^T} \mathcal{K}_{h_b}^{(\Sigma)} - \mathcal{D}^{-1} \right) \mathbf{Y}_n$$

where $\mathcal{K}_{h_b}^{(\Sigma)} = \mathcal{D}^{-1/2} \mathcal{M}^{(h_b, \Sigma)} = \begin{pmatrix} D_\alpha^{-1/2} P_{h_b} & D_\beta^{-1/2} Q_{h_b} \\ -D_\alpha^{-1/2} Q_{h_b} & D_\beta^{-1/2} P_{h_b} \end{pmatrix}$. Let us evaluate

$$\mathcal{E}_{h_b}^{(\Sigma)} = \mathcal{K}_{h_b}^{(\Sigma)^T} \mathcal{K}_{h_b}^{(\Sigma)} - \mathcal{D}^{-1}; \quad (4.6)$$

$$\mathcal{E}_{h_b}^{(\Sigma)} = \begin{pmatrix} P_{h_b} D_\alpha P_{h_b} + Q_{h_b} D_\alpha Q_{h_b} - D_\alpha & \mathbf{0}_d \\ \mathbf{0}_d & P_{h_b} D_\beta P_{h_b} + Q_{h_b} D_\beta Q_{h_b} - D_\beta \end{pmatrix}.$$

Since P_{h_b} , Q_{h_b} , D_α and D_β are diagonal matrices and $P_{h_b}^2 + Q_{h_b}^2 = I_d$, then $\mathcal{E}_{h_b}^{(\Sigma)} = \mathbf{0}_{2d}$. \square

Theorem (3.6) for univariate case and its generalization (4.1) allow to conclude that, for Gaussian distributions, there exists a family of stable methods defined by $\mathbf{Y}_{n+1} = \tilde{\Psi}_{h_b}^{(b)}(\mathbf{Y}_n)$, $(b, h_b) \in \Omega$ such that the expectation of the random variable Δ_N is equal to zero. In the context of HMC two different criteria might be followed to pick the best approximation method within the above family:

1. enlarge h_b as much as possible increasing b taking into account that stability decreases when we approach the roots of $p_{h_b}^2 - 1 = 0$. The best choice corresponds to $(b, h_b) \in \Omega$ such that $p_{h_b}^2 = 0$. We find $b = b_{max} \approx 0.2008$ and $h_{b_{max}} \approx 1.3432$;
2. choose $(b, h_b) \in \Omega$ in order to minimize the leading error term $k_{3,1}^2 + k_{3,2}^2$ with $k_{3,1} = \frac{12b^2 - 12b + 2}{24}$ and $k_{3,2} = \frac{-6b + 1}{24}$. In this case the optimal choice corresponds to $b = b_{ML} \approx 0.1932$ (see [10]) and the resulting $\tilde{h}_{b_{ML}} \approx 0.6549$.

In our simulations, we will compare the performance of integrators built on both the approaches.

5. Numerical examples.

5.1. Bivariate distribution. As first example, the simple $d = 2$ dimensional test in [12] is proposed, in order to numerically show the energy-preserving property of the proposed splitting technique. Consider sampling two position variables $\mathbf{X} = [X_1 \ X_2]^T$ from a bivariate Gaussian distribution with means zero, standard deviations of one and correlation 0.95. Two corresponding momentum variables $\mathbf{P} = [P_1, P_2]$ defined to have a Gaussian distribution with means of zero, standard deviations of one and zero correlation, are introduced. We then define the Hamiltonian as

$$U(\mathbf{X}) + K(\mathbf{P}) = \frac{1}{2} \mathbf{X}^T S_{95}^{-1} \mathbf{X} + \frac{1}{2} \mathbf{P}^T \mathbf{P}, \quad S_{95} = \begin{pmatrix} 1 & 0.95 \\ 0.95 & 1 \end{pmatrix}.$$

In order to describe the problem with notations suitable for the application of the proposed procedure, we diagonalize the symmetric matrix $S_{95} = V^T D_\alpha V$ with V unitary matrix of eigenvectors. In so doing, the Hamiltonian can be written as

$$U(\mathbf{Q}) + K(\mathbf{P}) = \frac{1}{2} \mathbf{Q}^T D_\alpha^{-1} \mathbf{Q} + \frac{1}{2} \mathbf{P}^T \mathbf{P}, \quad D_\alpha = \begin{pmatrix} 0.05 & 0 \\ 0 & 1.95 \end{pmatrix}$$

with $\mathbf{Q} = V \mathbf{X}$. A trajectory based on the above Hamiltonian, such as might be used to propose a new state in the Hamiltonian Monte Carlo method, computed using $N = 25$ steps of Störmer-Verlet method (hereafter denoted with SV-method) with stepsize $h = 0.25$ ($T^* = 16.4323$), is compared with the trajectory evaluated with the same number of steps by splitting method in (4.4) (hereafter denoted with SP-method) with $h = h_{b_{ML}} \approx 0.6573$ ($T^* = 6.5729$). Figure 1, on the top, shows the approximation of the two coordinates of the position vector $\mathbf{X} = V^T \mathbf{Q}$ while, on the bottom, the two momentum coordinates.

Notice that, position and momentum variables of SV method move upwards, until they reach an upper bound, at which point the direction of the motion is reversed. SP method instead circles approximating $U(\mathbf{X})$ in the coordinate plane and $K(\mathbf{P})$ in the momentum plane. The evaluation of the Hamiltonian $H(\mathbf{Y}) = U(\mathbf{X}) + K(\mathbf{P})$ after each steps is reported in Figure 2. Of course, it is exactly preserved by SP method while the Hamiltonian along the SV trajectory stays bounded as, with the chosen value of $h = 0.25$, SV is stable. Notice that the error in Hamiltonian for SV assumes positive values more often than negative and, at the end of SV trajectory, is 0.2186; so if this trajectory were used for an HMC proposal, the probability to accept the end-point as the next state would be $\exp(-0.2186) = 0.8036$.

In the second test, SV trajectories are used within the HMC procedure described in [Algorithm 2.2](#), while SP method was implemented in a HMC algorithm more similar to [Algorithm 2.1](#) as checking for accepting/rejecting proposal is useless for an energy-preserving integrator. A Gaussian bivariate distribution for \mathbf{q} with a correlation of 0.98, stronger than the one used in the previous case, is considered. The Hamiltonian is given by

$$U(\mathbf{X}) + K(\mathbf{P}) = \frac{1}{2} \mathbf{X}^T S_{98}^{-1} \mathbf{X} + \frac{1}{2} \mathbf{P}^T \mathbf{P}, \quad S_{98} = \begin{pmatrix} 1 & 0.98 \\ 0.99 & 1 \end{pmatrix}.$$

The results of $L = 20$ HMC iterations using trajectories of $N = 10$ SV-steps with stepsize $h = 0.18$ ($T^* = 1.8$) and of the same number of iterations with $N = 1$ SP-steps with $h = h_{b_{max}} = 1.3432$ are compared in Figure 3. Three proposals were rejected by HMC algorithm when SV-method was adopted. In Figure 3 we display HMC samples of the target distribution, starting from $\mathbf{X}_0 = [0, 2]^T$, an initial position far from the mean of the target. We can see that HMC rapidly approaches areas of high density under the target distribution. The SV and SP behaviours within HCM are similar with remarkable saving in terms of both number of steps ($N = 1$ vs. $N = 10$) and computational time in checking for acceptance/rejection, when an SP energy-preserving splitting integrator is adopted.

5.2. Multivariate distribution. In this example, also taken from [\[12\]](#), we consider a $d = 100$ dimensional multivariate Gaussian distribution with potential energy function $\frac{1}{2} \mathbf{Q}^T D_\alpha^{-1} \mathbf{Q}$ in which the variables are independent, with means zero and standard deviations $\alpha_j = j/100$ for $j = 1, \dots, d$. Kinetic energy function $H(\mathbf{P}) = \frac{1}{2} \mathbf{P}^T \mathbf{P}$ is set as above. For HMC with SV method, trajectories with

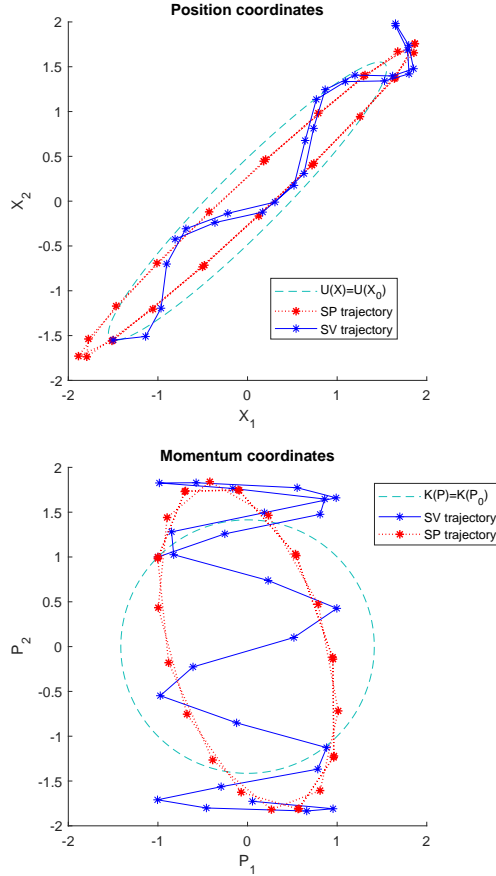


FIG. 1. Two trajectories for a bivariate Gaussian distribution (first test): 25 SV iterations with stepsize $h = 0.25$ (blue continuous line) and same number of iterations by means of SP splitting method with $h = \tilde{h}_{b_{ML}} \approx 0.6573$ (red dotted line). The initial state is $\mathbf{X}_0 = [-1.50, -1.55]^T$ and $\mathbf{P}_0 = [-1, 1]^T$. Position coordinates are drawn on the top while momentum coordinates are reported on the bottom. The underlying ellipses are $U(\mathbf{X}) = \frac{1}{2} \mathbf{X}^T S_{95}^{-1} \mathbf{X} = U(\mathbf{X}_0)$ (on the top) and $K(\mathbf{P}) = \frac{1}{2} \mathbf{P}^T \mathbf{P} = K(\mathbf{P}_0)$ (on the bottom).

$N = 150$ and h randomly selected, for each iteration, uniformly from the interval $(0.0104, 0.0156)$ are used ($T_{SV}^* \in (1.56, 2.34)$), while $N = \lfloor T_{SV}^* h_{b_{ML}} \rfloor \in \{2, 3\}$ is consequently randomly selected for SP method. Runs of $L = 1000$ iterations with both methods are computed and results are reported for comparison. The estimates for the mean and the standard deviations, evaluated as simple means and standard deviations of the values from the $L = 1000$ iterations for each of the $d = 100$ variables, against the theoretical values of standard deviations α_j , for $j = 1, \dots, d$, are shown in Figure 4. Notice that the error in the estimates for the means obtained with HMC algorithm with trajectories evaluated by both SP and SV methods are similar. Estimated values for the standard deviations with SP method appears even better then the ones provided by HMC with SV method. Of course, the saving in computational cost was very evident as, for each iteration, only $N = 2$ or $N = 3$ steps of SP method were necessary and all proposal accepted, despite the $N = 150$ steps

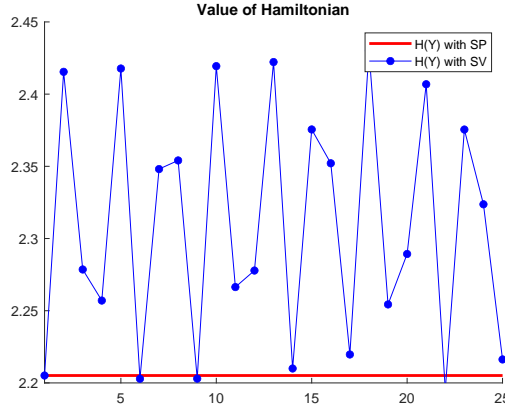


FIG. 2. *Bivariate distribution, first test.* The evaluation of the Hamiltonian $H(\mathbf{Y}) = \frac{1}{2} \mathbf{X}^T S_{95}^{-1} \mathbf{X} + \frac{1}{2} \mathbf{P}^T \mathbf{P}$ at each step with SV splitting method (blue dotted line) and the energy-preserving SP method (red continuous line).

used by SV method with 228 proposals rejected.

6. Conclusions. The very recent research literature on searching for efficient volume-preserving and reversible integrator able to replace the Störmer Verlet in the practical implementation of HMC method, uses as yardstick the ability of the numerical algorithm to reducing the expectation of the energy error variable when applied to univariate and multivariate Gaussian distributions [3],[2]. However, none of the above papers makes an explicit reference on the possibility to properly select the parameters in order to exactly preserve the Hamiltonian, as already done in the context of the geometric numerical integration [13], to nullify the expectation of the energy error.

In this paper, first steps along the above route, not previously beaten, are followed. A representation, different from the one given in [2], of linear maps corresponding to trajectories evaluated by mean of symplectic reversible splitting schemes for sampling from Gaussian distributions, was proposed. The formula for the expectation value of energy error is also deduced as in [2], in order to better appreciate similarities and differences with respect to the novel representation. In the proposed framework, the expression of the expectation value of the energy error puts in major evidence the role of the quantity which is the solely responsible for the distortion in calculated energy. Minimizing this quantity corresponds in reducing the number of rejections in practical implementation of HMC algorithm; consequently, methods with this quantity equal to zero are optimal for Gaussian univariate and multivariate distributions in terms of percent of accepted proposals.

In this paper, a class of optimal splitting methods for univariate and multivariate Gaussian distributions was built. As all proposals are accepted by construction, the numerical comparison is done with the Störmer-Verlet integrator, the only to beat as, in spite of the possible rejections, has a reduced number of composition of semiflows to be evaluated at each step, with respect to the proposed schemes. Indeed, the comparison with the other splitting integrators recently proposed in the literature [3], may have a little sense in that they are neither optimal for Gaussian distributions (as they are not energy-preserving methods) nor less expensive of the ones here considered.

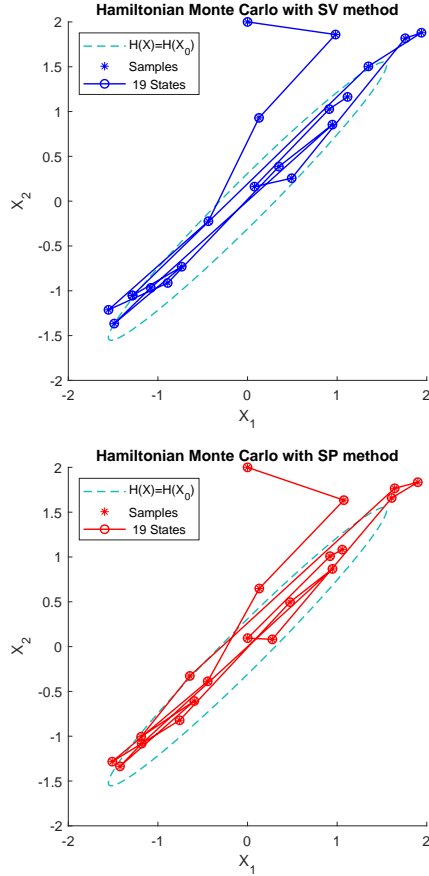


FIG. 3. *Bivariate distribution, second test. Iterations of HMC samples with 10 SV-steps, $h = 0.18$ (on the top) and one SP-step with $h = \tilde{h}_{b_{max}} \approx 1.3432$ (on the bottom) for the bivariate Gaussian distribution with correlation 0.98. The initial state is $\mathbf{x}^{(1)} = [0, 2]^T$ and $\mathbf{p}^{(1)} = [-1, 1]^T$. The plotted ellipses represents $U(\mathbf{X}) = \frac{1}{2} \mathbf{X}^T S_{98}^{-1} \mathbf{X} = U(\mathbf{X}_0)$, with $\mathbf{X}_0 = [-1.50, -1.55]^T$.*

The numerical experiments here performed are taken from [12] and intend to show, in a clear and simple way, the benefits of the novel proposed approach in solving Gaussian distribution rather than evaluating the performances on realistic (and more difficult to reproduce) examples. For these cases, further investigation is needed in determining the best choice of both parameter b and the final time T^* (or the number of steps N). The algorithm performance when using only one step ($N = 1$), suggests that a comparison with Langevin Monte Carlo method [7], [8] also deserves to be accomplished in future applications.

Unlike the proposed splitting schemes which are tailored for Gaussian distributions, the ones in [3], [2] have the advantage that they can be directly applied to more general distributions. The future challenge is hence to extend the presented framework for sampling from not Gaussian distributions. To this aim, a possible direction may be represented by the general idea given in [15], where the author proposed to approximate the potential energy by modelling it as a Gaussian process, that is inferred

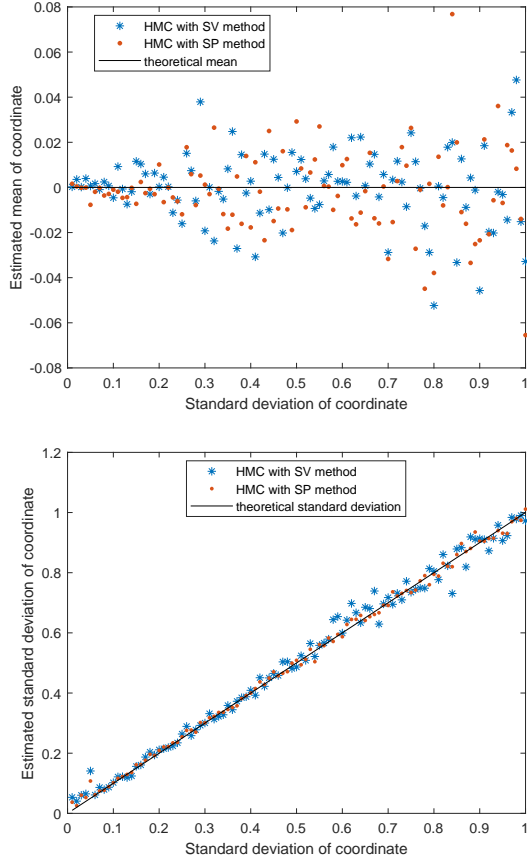


FIG. 4. *Multivariate distribution. Estimates of means (up) and standard deviations (down) for the $d = 100$ dimensional example. On the x-axes are reported the standard deviations α_j of each variable q_j for $j = 1, \dots, d$, on the y-axes the estimated values each evaluated from $L = 1000$ iterations, are reported.*

from values of the potential energy at positions selected during an initial exploratory phase [12]. This will be the focus of a future research work.

REFERENCES

- [1] B. J. ALDER AND T. E. WAINWRIGHT, *Studies in molecular dynamics. i. general method*, The Journal of Chemical Physics, 31 (1959), pp. 459–466.
- [2] S. BLANES, F. CASAS, AND J. SANZ-SERNA, *Numerical integrators for the Hybrid Monte Carlo method*, SIAM Journal on Scientific Computing, 36 (2014), pp. A1556–A1580.
- [3] M. P. CALVO, D. SANZ-ALONSO, AND J. SANZ-SERNA, *Hmc: avoiding rejections by not using leapfrog and some results on the acceptance rate*, arXiv preprint arXiv:1912.03253, (2019).
- [4] S. DUANE, A. D. KENNEDY, B. J. PENDLETON, AND D. ROWETH, *Hybrid monte carlo*, Physics letters B, 195 (1987), pp. 216–222.
- [5] E. HAIRER, C. LUBICH, G. WANNER, ET AL., *Geometric numerical integration illustrated by the stormer-verlet method*, Acta numerica, 12 (2003), pp. 399–450.
- [6] B. JOO, B. PENDLETON, A. D. KENNEDY, A. C. IRVING, J. C. SEXTON, S. M. PICKLES, S. P. BOOTH, U. COLLABORATION, ET AL., *Instability in the molecular dynamics step of a hybrid monte carlo algorithm in dynamical fermion lattice qcd simulations*, Physical Review D, 62 (2000), p. 114501.

- [7] A. KENNEDY, *The theory of hybrid stochastic algorithms*, in Probabilistic methods in quantum field theory and quantum gravity, Springer, 1990, pp. 209–223.
- [8] B. LEIMKUHLER AND C. MATTHEWS, *Robust and efficient configurational molecular sampling via langevin dynamics*, The Journal of chemical physics, 138 (2013), p. 05B601_1.
- [9] B. LEIMKUHLER AND S. REICH, *Simulating hamiltonian dynamics*, no. 14, Cambridge university press, 2004.
- [10] R. I. McLACHLAN, *On the numerical integration of ordinary differential equations by symmetric composition methods*, SIAM Journal on Scientific Computing, 16 (1995), pp. 151–168.
- [11] N. METROPOLIS, A. W. ROSENBLUTH, M. N. ROSENBLUTH, A. H. TELLER, AND E. TELLER, *Equation of state calculations by fast computing machines*, The journal of chemical physics, 21 (1953), pp. 1087–1092.
- [12] R. M. NEAL ET AL., *Mcmc using hamiltonian dynamics*, Handbook of markov chain monte carlo, 2 (2011), p. 2.
- [13] B. PACE, F. DIELE, AND C. MARANGI, *Splitting schemes and energy preservation for separable hamiltonian systems*, Mathematics and Computers in Simulation, 110 (2015), pp. 40–52.
- [14] C. PREDESCU, R. A. LIPPERT, M. P. EASTWOOD, D. IERARDI, H. XU, M. Ø. JENSEN, K. J. BOWERS, J. GULLINGSRUD, C. A. RENDLEMAN, R. O. DROR, ET AL., *Computationally efficient molecular dynamics integrators with improved sampling accuracy*, Molecular Physics, 110 (2012), pp. 967–983.
- [15] C. E. RASMUSSEN, *Gaussian processes to speed up hybrid monte carlo for expensive bayesian integrals*, in Seventh Valencia international meeting, dedicated to Dennis V. Lindley, Oxford University Press, 2003, pp. 651–659.
- [16] T. TAKAISHI AND P. DE FORCRAND, *Testing and tuning symplectic integrators for the hybrid monte carlo algorithm in lattice qcd*, Physical Review E, 73 (2006), p. 036706.